ParCYCLIC: Finite Element Modeling of Earthquake Liquefaction Response on Parallel Computers

Jun Peng[1], Jinchi Lu[2], Kincho H. Law[3] and Ahmed Elgamal[4]

Abstract

This paper presents the computational procedures and solution strategy employed in ParCYCLIC, a parallel nonlinear finite element program developed based on an existing serial code CYCLIC for the analysis of cyclic seismically-induced liquefaction problems. In ParCYCLIC, finite elements are employed within an incremental plasticity, coupled solid-fluid formulation. A constitutive model developed for simulating liquefaction-induced deformations is a main component of this analysis framework. The elements of the computational strategy, designed for distributed-memory message-passing parallel computer systems, include: (a) an automatic domain decomposer to partition finite element mesh; (b) nodal ordering strategies to minimize storage space for matrix coefficients; (c) an efficient scheme for the allocation of sparse matrix coefficients among the processors; and (d) a parallel sparse direct solver. Application of ParCYCLIC to simulate 3-D geotechnical experimental models is demonstrated. Not only good agreement is achieved between the computed and recorded results, but also the computational results show excellent parallel performance and scalability of ParCYCLIC on parallel computers with large number of processors.

Keywords

Parallel computation, sparse matrix, finite element modeling, earthquake liquefaction, domain decomposition

[1] Research Associate, Department of Civil and Environmental Engineering, Stanford University, Stanford, CA 94305. Phone: (650) 725-1886, Fax: (650) 723-4806, E-mail: junpeng@stanford.edu.

[2] Ph.D. Candidate, Department of Structural Engineering, University of California, San Diego, CA 92093. E-mail: jinlu@ucsd.edu.

[3] Professor, Department of Civil and Environmental Engineering, Stanford University, Stanford, CA 94305. E-mail: law@stanford.edu.

[4] Professor, Department of Structural Engineering, University of California, San Diego, CA 92093. E-mail: elgamal@ucsd.edu.

1 Introduction

Soil liquefaction is a complex phenomenon that causes many damages during earthquakes. The use of finite element methods for the simulations of earthquake response and liquefaction effects requires significant amount of execution time due to the complexity involved in coupling solid and fluid, as well as the need for sophisticated soil plasticity models. Large-scale earthquake simulations often exceed the capacity of current single-processor computers. Utilization of parallel computers with multiple processing and memory units can potentially reduce the solution time and allow analysis of large and complex models. Sequential application software, such as traditional finite element programs, needs to be re-designed in order to take full advantage of parallel computers.

Many structural and geotechnical analysis programs have been implemented on parallel computers. Since the most time consuming operation of a typical finite element analysis is the solution of linear simultaneous equations, some research efforts in the parallelization of finite element programs have been attempted on developing parallel equation solvers [1]. Parallel sparse direct solution techniques have been developed [2-7]. Various aspects of the parallel direct sparse solver implementations, including symbolic factorization, appropriate data structures, and numerical factorization, have been studied. This paper focuses on direct solution method for symmetric matrices. Specifically, a square-root free parallel LDL^T factorization, which can be applied to symmetric matrices containing negative diagonal entries, is presented.

There have also been many efforts on the implementation of nonlinear finite element analysis on distributed memory parallel computers. Watson and Noor presented a computational strategy for the nonlinear static and post-buckling analysis of large complex structures using nested dissection ordering scheme [8]. Gummadi and Palazotto described a nonlinear finite element formulation for beams and arches on a parallel machine [1]. They employed the concept of loop splitting to parallelize the element stiffness matrix generation. Nikishkov et al. presented a semi-implicit finite element code ITAS3D using domain decomposition method and direct solution method on a IBM SP2 computer, and reported that the parallel implementation was scalable to only a moderate number (up to 8) of processors [9]. Rometo et al. studied the nonlinear analysis of reinforced concrete three-dimensional frames on different parallel architectures, including a cluster of personal computers [10]. Modak and Sotelino presented an objected-oriented programming framework for parallel dynamic analysis of structures [11]. McKenna also presented a parallel object-oriented programming framework and a dynamic load balancing scheme to allow elements migrate between subdomains to reduce the number of wasted CPU cycles [12]. Krysl and Bittnar presented a nonlinear finite element program for explicit time integration of the momentum equations in structural dynamics [13]. Bao et al. modeled earthquake ground motion in large sedimentary basins using a 3D linear finite element program with explicit integration method on parallel computers and concluded that implicit method is not attractive on distributed memory computers [14].

This research presents the implementation of a parallel version of a geomechanics nonlinear finite element program for the simulation of earthquake ground response and liquefaction effects. The implementation is based on the serial program CYCLIC, which is a nonlinear finite element program developed to analyze cyclic mobility and liquefaction problems [15, 16]. Extensive calibration of CYCLIC has been conducted with results from experiments and full-scale response of earthquake simulations involving ground liquefaction. CYCLIC program is re-designed and parallelized to form ParCYCLIC. A parallel sparse direct solver has been incorporated to improve the simulation performance. The objectives of developing ParCYCLIC are to extend the computational capabilities of the finite element program to simulate large-scale systems, and to broaden the scope of its applications to seismic ground-foundation interaction problems.

2 Theoretical Background of ParCYCLIC

The finite element formulation and the stress-strain model adopted in ParCYCLIC are the same as those in CYCLIC. The theoretical development is based on the two phase (solid-fluid) fully-coupled finite element formulation of Chan [17] and Zienkiewicz et al. [18]. The soil constitutive model incorporated is developed specifically for liquefaction analysis [15, 19]. The current implementation is based on small-deformation theory and does not account for nonlinear effects due to finite deformation or rotation. In the following, the finite element formulation and the soil constitutive model adopted in CYCLIC and ParCYCLIC are briefly described.

2.1 Finite Element Formulation

In CYCLIC and ParCYCLIC, the saturated soil system is modeled as a two-phase material based on the Biot theory [20] for porous media. A numerical formulation of this theory, known as *u*-*p* formulation (in which displacement of the soil skeleton *u*, and pore pressure *p*, are the primary unknowns [17, 18]), is implemented [15, 16, 19]. This implementation is based on the following assumptions: small deformation and rotation, constant density of the solid and fluid in both time and space, locally homogeneous porosity which is constant with time, incompressibility of the soil grains, and equal accelerations for the solid and fluid phases.

The *u-p* formulation is defined by Chan [17] as two equations: one is the equation of motion for the solid-fluid mixture, and the other is the equation of mass conservation for the fluid phase that incorporates equation of motion for the fluid phase and Darcy's law. These two governing equations can be expressed in the following finite element matrix form [17]:

$$\mathbf{M\ddot{U}} + \int_{\mathbf{\Omega}} \mathbf{B}^{\mathbf{T}} \boldsymbol{\sigma}' \mathbf{d\Omega} + \mathbf{Qp} - \mathbf{f}^{s} = \mathbf{0} \tag{1a}$$

$$\mathbf{Q}^{\mathbf{T}} \mathbf{\dot{U}} + \mathbf{S\dot{p}} + \mathbf{Hp} - \mathbf{f}^{\mathbf{p}} = \mathbf{0} \tag{1b}$$

where **M** is the total mass matrix, **U** the displacement vector, **B** the strain-displacement matrix, $\boldsymbol{\sigma}'$ the effective stress vector (determined by the soil constitutive model described below), **Q** the discrete gradient operator coupling the solid and fluid phases, **p** the pore pressure vector, **S** the compressibility matrix, and **H** the permeability matrix. The vectors $\mathbf{f}^{s}$ and $\mathbf{f}^{\mathbf{p}}$ represent the effects of body forces and prescribed boundary conditions for the solid-fluid mixture and the fluid phase, respectively.

In Equation 1a (equation of motion), the first term represents inertia force of the solid-fluid mixture, followed by internal force due to soil skeleton deformation, and internal force induced by pore-fluid pressure. In Equation 1b (equation of mass conservation), the first two terms represent the rate of volume change for the soil skeleton and the fluid phase respectively, followed by the seepage rate of the pore fluid. Equations 1a and 1b are integrated in the time space using a single-step predictor multi-corrector scheme of the Newmark type [15, 17]. In the current implementation, the solution is obtained for each time step using the modified Newton-Raphson approach [15].

2.2 Soil Constitutive Model

The second term in Equation 1a, which corresponds to the internal force due to soil deformation, is defined by the soil stress-strain constitutive model. The finite element program incorporates a soil constitutive model [15, 16, 21] based on the original multi-surface-plasticity theory for frictional cohesionless soils [22]. This model was developed with emphasis on simulating the liquefaction-induced shear strain accumulation mechanism in clean medium-dense sands [16, 21, 23, 24]. Special attention was given to the deviatoric-volumetric strain coupling (dilatancy) under cyclic loading, which causes increased shear stiffness and strength at large cyclic shear strain excursions (i.e., cyclic mobility).

The constitutive equation is written in incremental form as follows [22]:

$$\dot{\boldsymbol{\sigma}}' = \boldsymbol{E} : (\dot{\boldsymbol{\varepsilon}} - \dot{\boldsymbol{\varepsilon}}^{p}) \tag{2}$$

where $\dot{\boldsymbol{\sigma}}'$ is the rate of effective Cauchy stress tensor, $\dot{\boldsymbol{\varepsilon}}$ the rate of deformation tensor, $\dot{\boldsymbol{\varepsilon}}^{p}$ the plastic rate of deformation tensor, and $\boldsymbol{E}$ the isotropic fourth-order tensor of elastic coefficients. The rate of plastic deformation tensor is defined by: $\dot{\boldsymbol{\varepsilon}}^{p}$ = **P** $\langle L \rangle$, where **P** is a symmetric second-order tensor defining the direction of plastic deformation in stress space, *L* the plastic loading function, and the symbol $\langle\ \rangle$ denotes the McCauley's brackets (i.e., $\langle L \rangle$=max(*L*, 0)). The loading function *L* is defined as: *L* = $\mathbf{Q}{:}\dot{\boldsymbol{\sigma}}'/H'$ where H' is the plastic modulus, and **Q** a unit symmetric second-order tensor defining yield-surface normal at the stress point (i.e., **Q**= $\nabla f / \|\nabla f\|$), with the yield function f written in the following form:

$$f = \frac{3}{2}(\boldsymbol{s} - (p' + p'_0)\boldsymbol{\alpha}) : (\boldsymbol{s} - (p' + p'_0)\boldsymbol{\alpha}) - M^2 (p' + p'_0)^2 = 0 \qquad (3)$$

in the domain of $p' \geq 0$ [21]. The yield surfaces in principal stress space and deviatoric plane are shown in Figure 1. In Equation 3, $\boldsymbol{s} = \boldsymbol{\sigma}' - p'\boldsymbol{\delta}$ is the deviatoric stress tensor, p' the mean effective stress, p'_0 a small positive constant (1.0 kPa in this paper) such that the yield surface size remains finite at $p' = 0$ for numerical convenience (Figure 1), $\boldsymbol{\alpha}$ a second-order kinematic deviatoric tensor defining the surface coordinates, and *M* dictates the surface size. In the context of multi-surface plasticity, a number of similar surfaces with a common apex form the hardening zone (Figure 1). Each surface is associated with a constant plastic modulus. Conventionally, the low-strain (elastic) module and the plastic module are postulated to increase in proportion to the square root of p' [22].

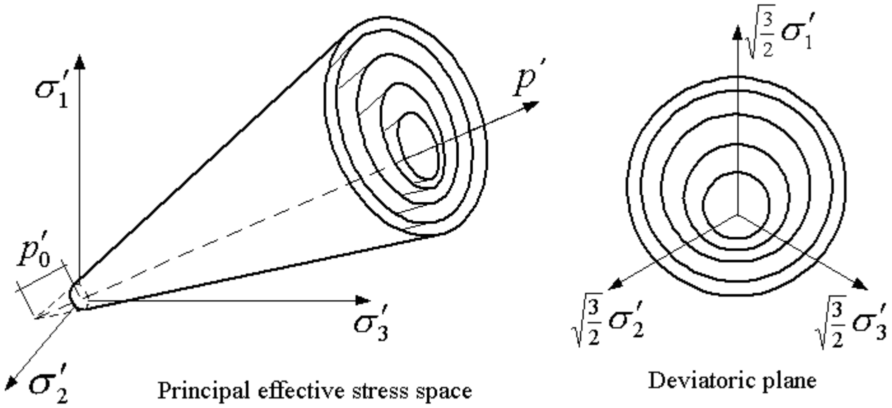
σ'_1
p'
p'_0
σ'_3
σ'_2
Principal effective stress space
$\sqrt{\frac{3}{2}}\sigma'_1$
$\sqrt{\frac{3}{2}}\sigma'_2$
$\sqrt{\frac{3}{2}}\sigma'_3$
Deviatoric plane

Figure 1. Conical Yield Surfaces for Granular Soils in Principal Stress Space and Deviatoric Plane

The flow rule is chosen so that the deviatoric component of flow **P′** = **Q′** (associative flow rule in the deviatoric plane) and the volumetric component P'' define the desired amount of dilation or contraction in accordance with experimental observations. Consequently, P'' defines the degree of non-associativity of the flow rule and is given by Parra [15] as follows:

$$P'' = \frac{(\eta/\overline{\eta})^2 - 1}{(\eta/\overline{\eta})^2 + 1}\Psi \tag{4}$$

where $\eta = ((3/2)\boldsymbol{s}:\boldsymbol{s})^{1/2}/p'$ is effective stress ratio, $\overline{\eta}$ a material parameter defining the stress ratio along the phase transformation (PT) surface [25], and Ψ a scalar function controlling the amount of dilation or contraction depending on the level of confinement and/or cumulated plastic deformation [21]. The sign of $(\eta/\overline{\eta})^2 - 1$ dictates dilation or contraction: if the sign is negative, the stress point lies below the PT surface and contraction takes place (phase 0-1, Figure 2); otherwise, if the sign is positive, the stress point lies above the PT surface and dilation occurs under shear loading (phase 2-3, Figure 2). At low confinement levels, accumulation of plastic deformation may be prescribed (phase 1-2, Figure 2) before the onset of dilation [21].

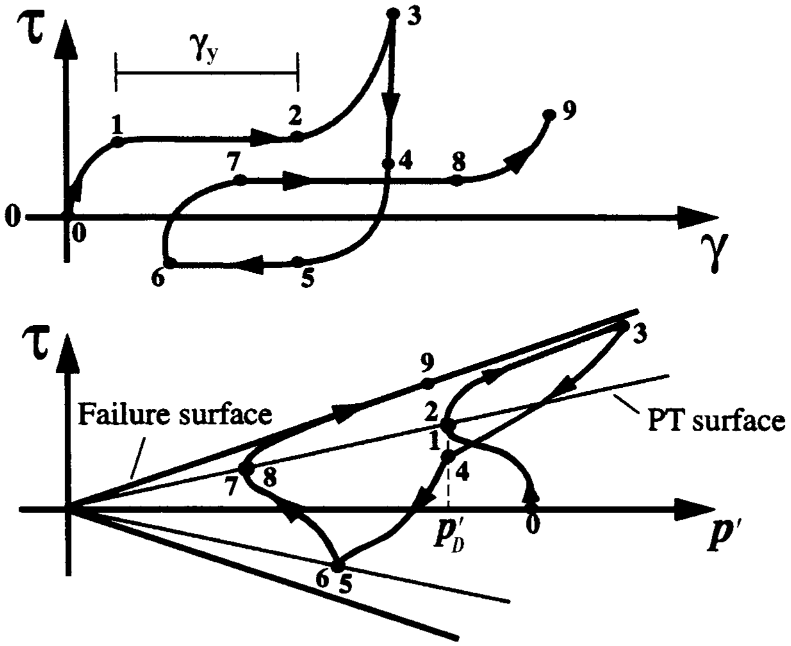

Figure 2. Shear Stress-Strain and Effective Stress Path under Undrained Shear Loading Conditions

A purely deviatoric kinematic hardening rule is chosen according to Prevost [22]:

$$p' \dot{\boldsymbol{\alpha}} = b \, \boldsymbol{\mu} \tag{5}$$

where $\boldsymbol{\mu}$ is a deviatoric tensor defining the direction of translation and b is a scalar magnitude dictated by the consistency condition. In order to enhance computational efficiency, the direction of translation $\boldsymbol{\mu}$ is defined by a new rule [15, 21], which maintains the concept of conjugate-points contact by Mroz [26]. Thus, all yield surfaces may translate in stress space within the failure envelope

3 ParCYCLIC Software Organization

3.1 Parallel Program Strategies

Programming models required to take advantage of parallel computers are significantly different from the traditional paradigm for a sequential program [27]. In a parallel computing environment, cares must be taken to maintain all participating processors busy performing useful computations and to minimize communication among the processors. To take advantage of parallel processing power, the algorithms and data structures of CYCLIC are re-designed and implemented in ParCYCLIC.

One approach in developing application software for distributed memory parallel computers is to use the single-program-multiple-data (SPMD) paradigm [28, 29]. The SPMD paradigm is related to the *divide and conquer* strategy and is based on breaking a large problem into a number of smaller sub-problems, which may be solved separately on individual processors. In this parallel programming paradigm, all processors are assigned the same program code but run with different data sets comprising the problem. A finite element domain is first decomposed using some well-known domain decomposition techniques. Each processor of the parallel machine then solves a partitioned domain, and data communications among sub-domains are performed through message passing. Domain decomposition is attractive in finite element computations on parallel computers because it allows individual sub-domain operations to be performed concurrently on separate processors. The SPMD model has been applied successfully in the development of many parallel finite element programs from legacy serial codes [28, 30]. The development of ParCYCLIC follows the SPMD model to parallelize the legacy serial code CYCLIC.

3.2 Computational Procedures

The computational procedure of ParCYCLIC is illustrated in Figure 3. The procedure can be divided into three phases, namely: preprocessing and input phase, nonlinear solution phase, and output and postprocessing phase. The first phase consists of initializing certain variables, allocating memories, and reading the input file. There is no inter-process communication involved in this phase – all the processors run the same piece of code and read identical copies of the same input file. Since a mesh partitioning routine is incorporated in ParCYCLIC, the input file does not need to contain any information for processor assignment of nodes and elements. The input file for ParCYCLIC has essentially the same format as that of CYCLIC.

After the preprocessing and input phase, the nonlinear solution phase starts with using a domain decomposer to partition the finite element mesh. Symbolic factorization is then performed to determine the nonzero pattern of the matrix factor. After the symbolic factorization, the storage spaces for the sparse matrix factor required by each processor are allocated. Since all the processors need to know the nonzero pattern of the global stiffness matrix and symbolic factorization generally only takes a small portion of the total runtime, each processor carries out the domain decomposition and symbolic factorization based on the global data.

In the nonlinear analysis solution phase, the program essential goes through a while loop until the number of increments reaches the pre-set limit or errors/exceptions are being encountered inside the loop. In the nonlinear solution phase, modified Newton-Raphson algorithm is employed, that is, the stiffness matrix at each iteration step uses the same tangential stiffness from the initial step of the increment. For large-scale finite element modeling, the global matrix assembly and numerical factorization require substantial computation and message exchange. Although the modified iterative approach typically requires more steps per load increment as compared with full Newton-Raphson scheme, substantial savings can be realized as a result of not having to assemble and factorize a new global stiffness matrix during each iteration step. In ParCYCLIC, there is one variation to the typical modified Newton-Raphson algorithm. As shown in Figure 3, a convergence test is performed at the end of each iteration step. If the solution is not converged after a certain number of iterations (e.g., 10 iterations) within a particular time step, the time step will be divided into two to expedite convergence. This process repeats until the solution converges.

The numerical solution scheme for the linear system of equations $Kx = f$ in ParCYCLIC is based on the row-oriented parallel sparse solver developed by Mackay and Law [7]. The direct solution of the linear system of equations consists of three steps: (1) parallel factorization of the symmetric matrix K into its matrix product LDL^T; (2) parallel forward solution, $y = L^{-1} f$; and (3) parallel backward substitution, $x = L^{-T} D^{-1} y$.

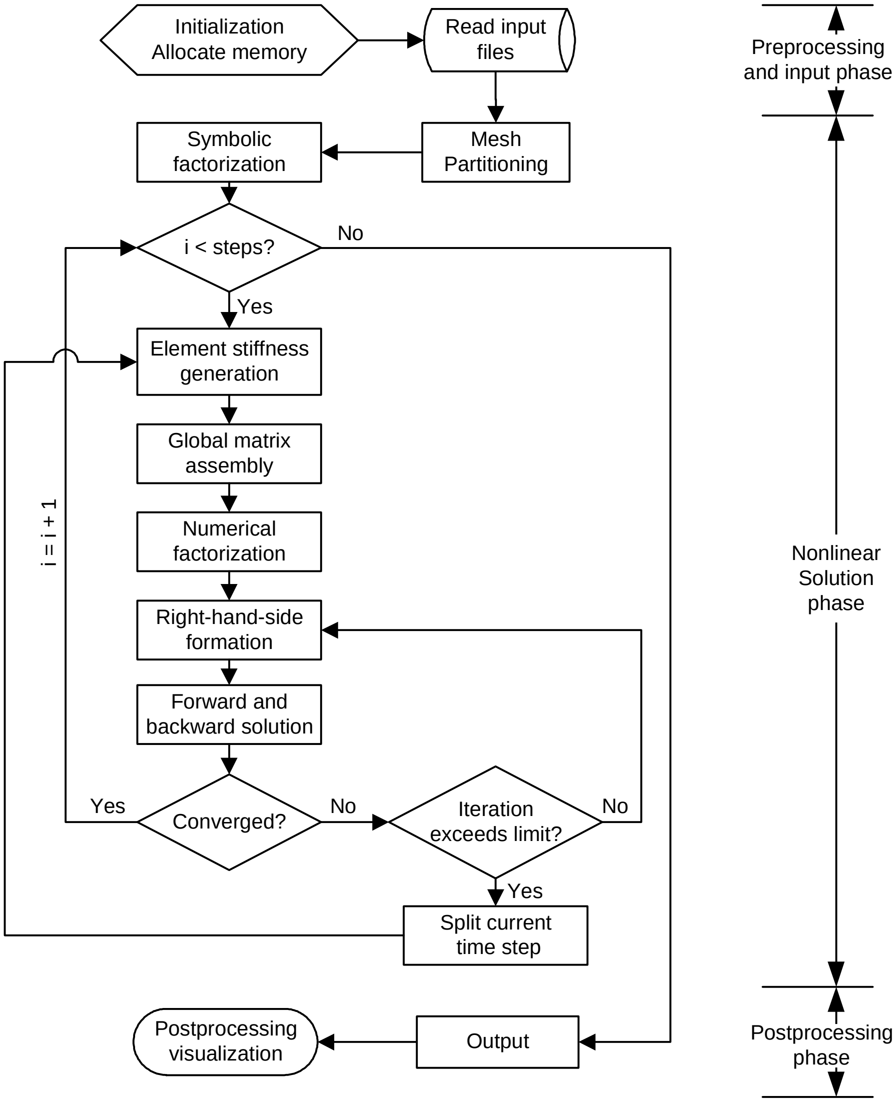

Figure 3. Flowchart of Computational Procedures in ParCYCLIC

The final phase, output and postprocessing, consists of collecting the calculated node response quantities (e.g. displacements, acceleration, pore pressure, etc.) and element output (such as normal stress, normal strain, volume strain, shear strain, mean effective stress, etc.) from the different processors. The response quantities and timing results are then written into files for future processing and visualization.

3.3 Message Exchange Using MPI

During the parallel execution of ParCYCLIC, processors in the program need to communicate with each another. The inter-processor communication of ParCYCLIC is implemented using MPI (Message Passing Interface) [31], which is a specification of a standard library for message passing. MPI was defined by the MPI Forum, a broadly based group of parallel computer vendors, library developers, and applications specialists. One advantage of MPI is its portability, which makes it suitable to develop programs to run on a wide range of parallel computers and workstation clusters. Another advantage of MPI is its performance, because each MPI implementation is optimized for the hardware it runs on. Generally, MPI code can be developed for an arbitrary number of processors. It is up to the users to decide, at run-time, how many processors should be invoked for the execution.

The MPI library consists of a large set of message passing primitives (functions) to support efficient parallel processes running on a large number of processors interconnected over a network. The implementation of ParCYCLIC employs only a small set of MPI message passing functions. There are two types of communications in ParCYCLIC: point-to-point communication and collective messages. The point-to-point communication in MPI involves the transmittal of data between two processors. The collective communications, on the other hand, transmit data among all processors in a group.

For the implementation of ParCYCLIC, point-to-point messages are used extensively during the global matrix assembly and matrix factorization phases. Figure 4 shows some sample codes for the point-to-point messages in ParCYCLIC, which have the following features:

- For most of the point-to-point communications, the blocking send (`MPI_Send`) is used to send out data, and the non-blocking receive (`MPI_Irecv`) is used to receive data. The purpose of this choice is to keep all the processors busy performing useful computation and at the same time to ensure all the messages are delivered. A blocking send temporarily stores the message data in a buffer. The function does not return until the message has been safely delivered. A non-blocking receive tests the buffer for any incoming messages, and can concurrently perform computation not relying on the incoming messages.

- The `MPI_Send` sends a message to the specific recipient by passing the receiver's node identification (denoted as `r_node` in Figure 4) as one of the parameters. The `MPI_Irecv`, on the other hand, receives a message from any source by denoting the sender as a wild card value of `MPI_ANY_SOURCE`. The sender knows whom the recipient is when sending a particular message, while the receiver listens to messages from all processors. After a message is received, the `MPI_SOURCE` field of the `MPI_Status` is retrieved to find the node identification of the sender. The actual size of the received message is detected by calling the function `MPI_Get_count`.

- Instead of sending messages with data type information (such as double, integer, byte, etc.), all data are sent as a byte stream, which is denoted as `MPI_BYTE`. Since messages have overhead cost, minimizing the number of messages improves the system performance. One way to reduce the number of messages is for the sender to combine messages. Each sender maintains a buffer for all the outgoing messages, and these messages will not be sent off to other processors unless the buffer is nearly full. Since the buffer may contain mixted types of data, the byte stream is a common format to represent the content of the buffer. The type information of the actual content can be retrieved during the unpacking of a message according to the pre-defined communication protocol.

```
MPI_Request request;
MPI_Status status;
int mlen;
int s_node, r_node;

MPI_Send(sendbuf, len, MPI_BYTE, r_node, tag, MPI_COMM_WORLD);

MPI_Wait(&request, &status);

/* set up recbuf for the incoming message*/
...
MPI_Irecv(recbuf, length, MPI_BYTE, MPI_ANY_SOURCE, tag,
          MPI_COMM_WORLD, &request);

s_node = status.MPI_SOURCE;
MPI_Get_count(&status, MPI_BYTE, &mlen);
Unpack(recbuf, mlen);
```

Figure 4. Sample Code for Point-to-Point Message in ParCYCLIC

There are three types of collective communications in the implementation of ParCYCLIC: barrier synchronization, gather-to-all, and broadcast. The barrier synchronization function, `MPI_Barrier`, blocks the caller until all processors within a group have finished calling it. The barrier synchronization can be used to ensure all the processors are at the same pace.

The gather-to-all function is employed for performing a global operation (such as sum, max, logical, and etc.) across all the processors of a group. The gather-to-all function is applied in ParCYCLIC to gather global information. For example, since each processor is working on a portion of the domain, it only holds the solution for that portion. A gather-to-all function call is needed at the end of the numerical solution phase to collect the global solution from each processor. The gather-to-all function, `MPI_Allreduce`, has the following syntax:

```
MPI_Allreduce(sendbuf, recvbuf, count, [MPI_INT, MPI_DOUBLE...],
              [MPI_MAX, MPI_MIN, MPI_SUM...], MPI_COMM_WORLD);
```

The third type of collective messages is broadcast, which sends a message to all the members of a processors group. In ParCYCLIC, most communications in forward and backward solution phase require sending the same message to more than one processor. Figure 5 shows some sample codes for broadcasting messages in ParCYCLIC. After knowing which processor belongs to the broadcast group, the `MPI_Comm_create` function can be invoked to create a communication group `MPI_Comm`. The group communication is then handled by a broadcast message to the `MPI_Comm`.

```
int *sendlist, nshare;
MPI_Comm workers;
MPI_Group world_group, worker_group;

MPI_Comm_group(MPI_COMM_WORLD, &world_group);
MPI_Group_incl(world_group, nshare, sendlist, &worker_group);
MPI_Comm_create(MPI_COMM_WORLD, worker_group, &workers);

MPI_Bcast(buf, length, MPI_BYTE, my_pid, workers);
```

Figure 5. Sample Code for Broadcast Message in ParCYCLIC

4 Parallel Sparse Direct Solver

For nonlinear finite element analysis, the assembly to and the solution of the global matrix consume the greatest share of the computation effort [32]. Therefore, parallelizing these two parts has significant overall performance benefits. A parallel row-oriented sparse solution method for finite element analysis [7] has been enhanced and implemented in ParCYCLIC.

4.1 Mesh Partitioning Using Domain Decomposition

In a parallel sparse solver, a domain decomposer is needed to partition the finite element mesh into subdomains. To achieve high parallel efficiency of the parallel solver, it is important that the finite element mesh is partitioned in such a way that computational workloads are well balanced among processors and inter-processor communication is minimized.

To decompose a finite element domain, ParCYCLIC employs METIS, which is a software package for partitioning large irregular graphs, partitioning large meshes, and computing fill-reducing ordering of sparse matrices [33]. The algorithms in METIS are based on multilevel graph partitioning [34, 35]. The multilevel algorithm reduces the original graph partitioning problem to a sequence of bisection steps. That is, the algorithm first divides the graph into two pieces, and then recursively bisects the two sub-pieces independently. The multilevel partitioning method is quite different from traditional methods.

Traditional graph partitioning algorithms compute a partition of a graph by operating directly on the original graph. Multilevel partitioning algorithm, on the other hand, takes a different approach. First, the algorithm reduces the size of the graph by collapsing vertices and edges to produce a smaller graph. The graph partitioning is then performed on the collapsed graph. Finally, the partition is propagated back through the sequence to un-collapse the vertices and edges, with an occasional local refinement [33].

METIS provides both stand-alone programs (executable files) and library interfaces (functions). The library interfaces are incorporated in ParCYCLIC to perform the domain decomposition. In particular, multilevel *k*-way partitioning routine is used in ParCYCLIC to partition a graph into *k* parts. The number of processors (power of 2 is suggested) used in the execution of ParCYCLIC determines the number of levels to partition. The objective of the partitioning is to minimize the total communication volume. Once the cuts are found by METIS routines, i.e., the finite element mesh has been partitioned into subdomains, the internal nodes of each subdomain still need to be ordered to reduce the fill-ins of the matrix factors. There are many ordering routines implemented in ParCYCLIC to perform this task, including Reverse Cuthill-McKee [36], Minimum Degree [37], General Nested Dissection [38], and Multilevel Nested Dissection [34]. Users are allowed to choose different types of ordering routines for a specific problem. Otherwise, the default ordering routine is the Multilevel Nested Dissection ordering, because it is stable and normally generates an ordering with the least fill-ins of the matrix factors. After the matrix ordering is complete, symbolic factorization and parallel matrix assignment are performed.

4.2 Assignment of Sparse Stiffness Matrix

The notion of the elimination tree plays a significant role in sparse matrix study [39]. It is well known that the nonzero entries in the numerical factor *L* can be determined by the original nonzero entries of the stiffness matrix *K* [40, 41] and a list vector, which is defined as

$$PARENT(j) = \min\{i \mid L_{ij} \neq 0\} \tag{6}$$

The array *PARENT* represents the row subscript of the first nonzero entry in each column of the lower triangular matrix factor *L*. The definition of the list array *PARENT* results in a monotonically ordered elimination tree of which each node has its numbering higher than its descendants. By topologically post-ordering the elimination tree, the nodes in any subtree can be numbered consecutively. The resulting sparse matrix factor is partitioned into block submatrices where the columns/row of each block corresponds to the node set of a branch in the elimination tree. Figure 6 shows a simple square finite element grid and its post-ordered elimination tree representation. One important feature of the elimination tree is that it describes the dependencies among the variables during the factorization process.

That is, a column block may not be factored until all nodes below the nodes representing the column block have been factored. This implies that all the column blocks represented by the leaves of the elimination tree have no dependencies. These column blocks can be factored independently and concurrently.

The coefficients of a sparse matrix factor are distributively stored among the processors according to the column blocks. Figure 7 shows an example of the data assignment of a sparse matrix on four processors for the finite element model shown in Figure 6. The strategy is to assign the rows corresponding to the nodes along each branch of the elimination tree (column block) to a processor or a group of processors. Beginning at the root of the elimination tree, the nodes belonging to this branch of the tree are assigned among the available processors in a rotating round robin fashion. As we traverse down the elimination tree, at each fork of the elimination tree, the group of processors is divided to match the number and size of the subtrees below the current branch. A separate group of processors is assigned to each branch at the fork and the process is repeated for each subtree. The process of assigning groups of processors to each branch of the elimination tree continues until only one processor remains for the subtree. At this stage, all remaining nodes in the subtree are assigned to the single processor.

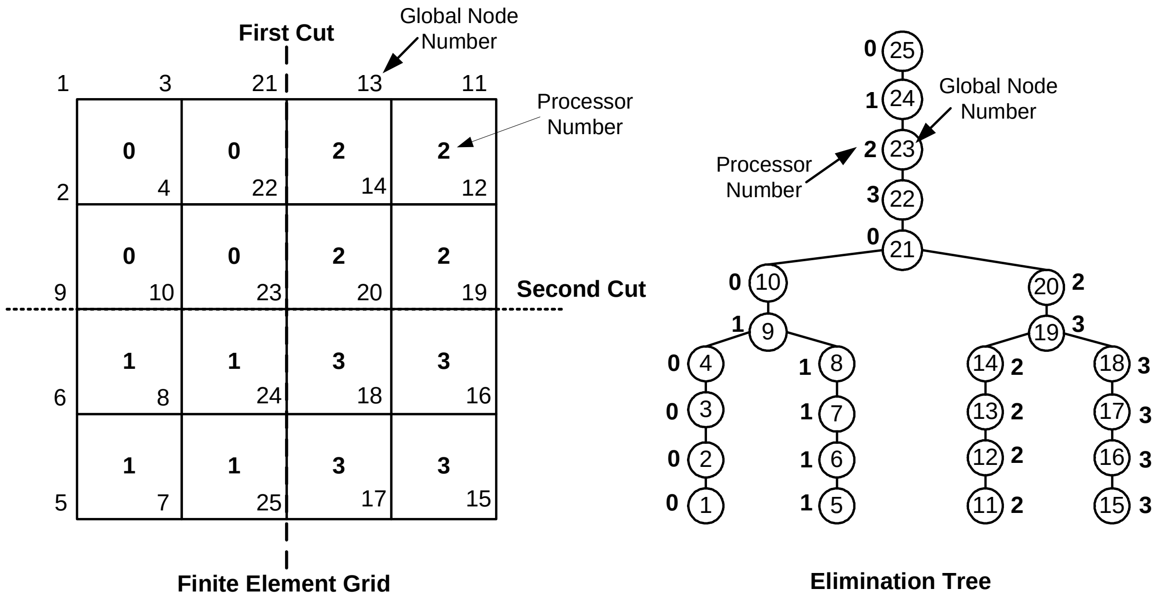

Figure 6. A Finite Element Grid and Its Elimination Tree Representation

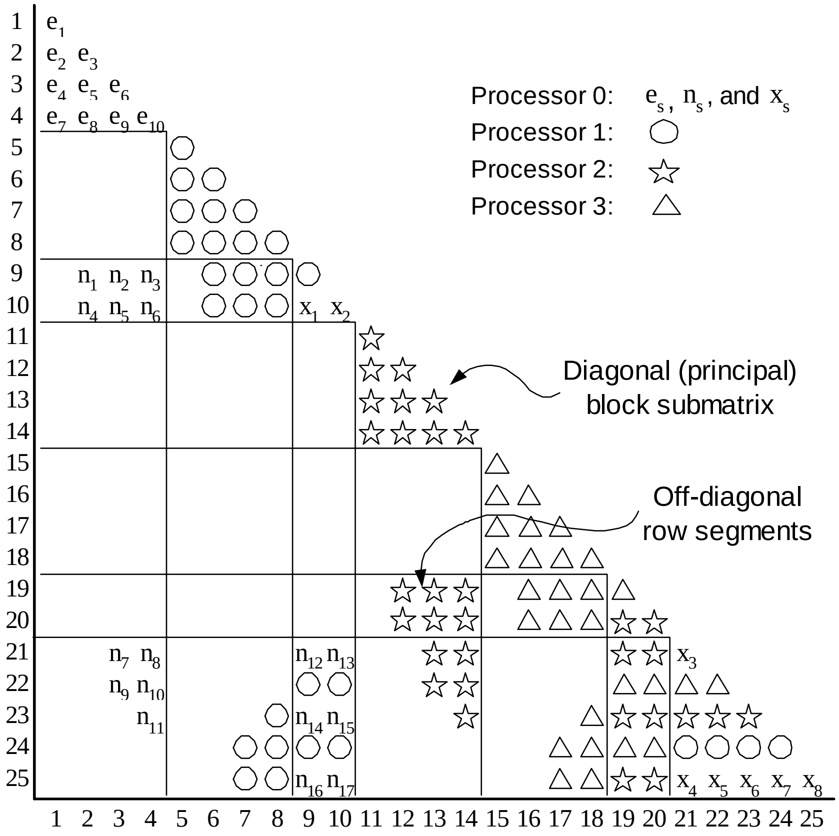
Processor 0: e_s, n_s, and x_s
Processor 1: ○
Processor 2: ☆
Processor 3: △
Diagonal (principal) block submatrix
Off-diagonal row segments

Figure 7. Matrix Partitioning for Parallel Computations

The matrix assignment strategy described partitions a sparse matrix into two basic sets: the principal diagonal block submatrices and the row segments outside the principal block submatrices. For the principal block submatrices, which have a profile structure, the processor assignment proceeds on a row group by row group basis with each row group corresponding to a node in the finite element model. This strategy divided the diagonal block submatrices into two groups: one is assigned to a single processor and the other is shared by multiple processors. For the row segments outside the diagonal blocks, the rows are assigned to the processors sharing the node set (column block) in rotating round robin fashion.

4.3 Data Structure for Matrix Coefficients

After the symbolic factorization, all the nonzero entries in the matrix factor are determined. The data structure for storing the matrix coefficients is directly set up for the factored matrix *L*. There are three different data structures for storing the coefficients: one for the principal block submatrices associated with the column blocks assigned to a single processor, one for the principal block submatrices associated with column blocks shared by multiple processors, and one for the row segments in column blocks. The following describes the details of these three different data structures. For demonstration purpose, the data structure in Processor 0 for the square grid problem shown in Figure 7 is presented.

The data structure for the principal block submatrices assigned to a single processor is illustrated in Figure 8. It consists of an array of pointers `ipenv` which points to the beginning of the coefficients for each row, and an array of integers to indicate the corresponding global row numbers. The actually matrix coefficients are stored consecutively to facilitate efficient access.

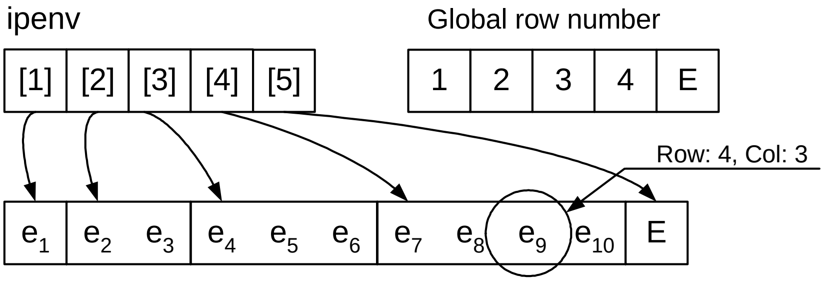

Figure 8. Data Structure for Principal Block Submatrix Assigned to a Single Processor

The data structure for the principle block submatrices assigned to multiple processors is illustrated in Figure 9. The array of pointers `epenv` points to the beginning coefficients of each row just like `ipenv` does for principal block submatrices assigned to a single processor. The global row numbers and the length of the rows are stored in another array for each row block. Because each row block ends with an element in the matrix diagonal, the row number and row length are sufficient to map a stored matrix coefficient to its location in the global matrix. For example, the matrix coefficient $\mathbf{X_7}$ belongs to the third row block, which has global row number of 25 and row length of 5. Since we know that $\mathbf{X_7}$ is the second to the last elements in the row block, the global column number for $\mathbf{X_7}$ can be calculated as to be 24.

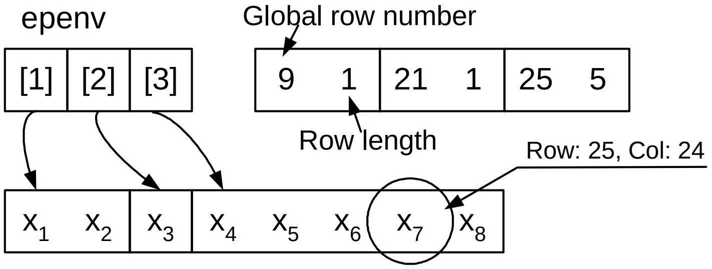

Figure 9. Data Structure for Principal Block Submatrix Shared by Multiple Processors

The third data structure stores the row segments, as illustrated in Figure 10. This data structure is essentially a linked list with each node corresponding to a row segment. Each node in the linked list contains four variables, namely the global row number, the starting global column number for the row segment, a pointer to the next node, and a pointer to the beginning of the matrix coefficients for the row segment. These variables can be used to find the global row number and column number of a particular matrix coefficient. For example, in Figure 10, the node in the linked list corresponding to matrix coefficient $\mathbf{n}_{15}$ has row number 23 and starting column number 9. Since $\mathbf{n}_{15}$ is the second element in the row segment, its column number can be calculated as 10.

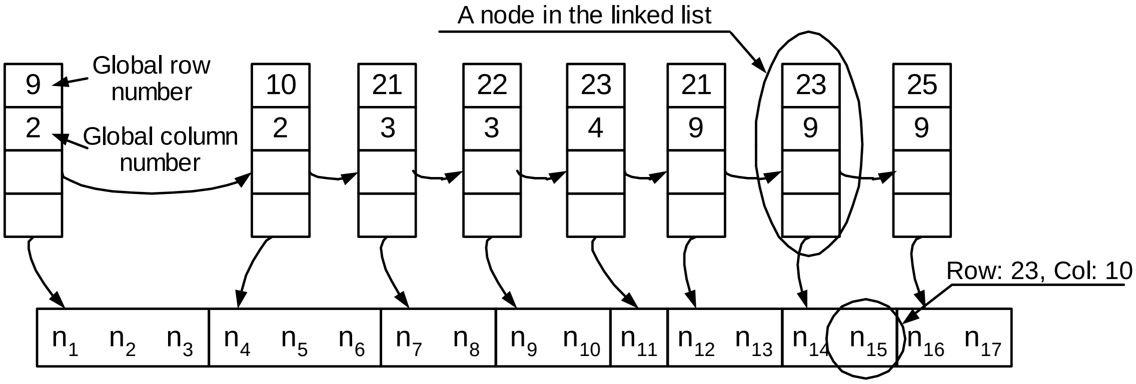
A node in the linked list
Global row number
Global column number
9
2
10
2
21
3
22
3
23
4
21
9
23
9
25
9
Row: 23, Col: 10
n_1 n_2 n_3 n_4 n_5 n_6 n_7 n_8 n_9 n_{10} n_{11} n_{12} n_{13} n_{14} n_{15} n_{16} n_{17}

Figure 10. Data Structure for Row Segments

4.4 Parallel Global Matrix Assembly

The generation of element stiffness matrices is one of the most natural tasks for parallel implementation. Since each element stiffness matrix can be generated independently of the other element stiffness matrices, each processor can work independently on the elements assigned to it. After the stiffness matrix of an element is generated, the processor that has the element assigned to it will be responsible to assemble the element coefficients to the matrix data structure described in the previous section. There are two strategies for assigning elements to different processors. For the first strategy, each element is assigned to a particular processor with no duplication of element assignment. The second strategy allows duplicated assignment of elements to the processors but requires no inter-processor communication for global matrix assembly.

The first strategy is to distribute the elements to different processors according to the processor assignment of the global nodal variables of the elements. This element assignment strategy can be summarized as follows [27]:

1. If all the nodal variables of an element belong to a single processor, the element is assigned to that processor.

2. If one of the nodal variables of an element belongs to a column block assigned to a single processor, then the element is assigned to that processor.

3. If all nodal variables of an element are shared among multiple processors, the element is assigned to the processor which is assigned the lowest global number variable of the element stiffness matrix.

For the parallel global matrix assembly, coefficients of the element stiffness matrices that belong to the processor where the element stiffness matrix is formed are assembled into the global stiffness matrix directly. If the coefficients of the element stiffness matrix belong to the segment of the global stiffness matrix located in another processor, they are sent to that processor for assembly.

The first element assignment strategy ensures no duplication of element stiffness generation, but substantial amount of messages are needed to exchange the stiffness matrix coefficients among the processors. To eliminate the messages for global matrix assembly, a second element assignment strategy is introduced in ParCYCLIC. All the elements along a cut are assigned to a group of processors that share the cut. In this strategy, the same element may be assigned to more than one processor, and consequently the element stiffness generation will be duplicated. However, the duplication of work can be offset by not having to exchange messages. During the global matrix assembly phase, coefficients of the element stiffness matrices that belong to the processor where the element stiffness matrix is formed are assembled into the global stiffness matrix directly. If the coefficients of the element stiffness matrix belong to another processor, they are simply discarded.

Both strategies for element assignment have been implemented in ParCYCLIC. For illustration purpose, Figure 11 shows the results of applying both strategies to assign elements to four processors for the square grid model. Depending on the characteristics of the finite element model, users can choose which strategy to be used. For large finite element models where the interface (cuts) is relatively small (in other words, most of the elements have all their nodes assigned to a single processor), strategy two is recommended. From the performance point of view, the performance overhead is small because the number of duplicated elements is only a small portion of the total number of elements. From the execution point of view, strategy two incurs no communication and thus easier to guarantee the completion of matrix assembly.

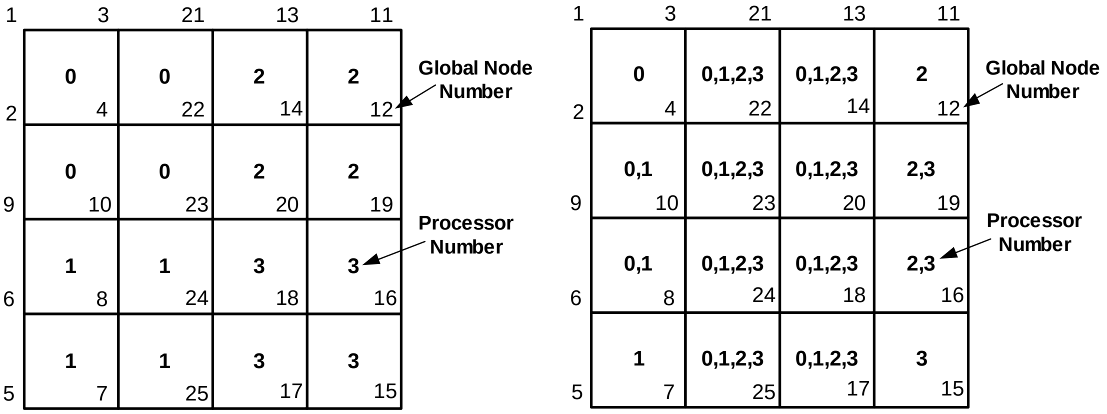

(a). Assignment of elements without duplication

(b). Assignment of elements with duplication

Figure 11. Two Methods of Assigning Elements to Four Processors

4.5 Parallel Numerical Factorization

Once the processor assignment and the assembly of the global stiffness matrix are completed, numerical calculation can proceed. In ParCYCLIC, the LDL^T factorization is performed. The parallel numerical factorization procedure is divided into two distinct phases. During the first phase, the column blocks assigned entirely to a single processor are factorized. The strategy is to carry out as much computation as possible in the local processor. Figure 12 shows the parallel factorization procedures in this phase with the factor of matrix coefficients in Processor 1 being highlighted. The operations in this phase are as follows:

1. For each column block assigned to a processor, perform a profile factorization on principal block submatrix.

2. Update the off-diagonal row segments below the principal submatrix by a series of forward solutions.

3. After the column blocks are factorized, form dot products among row segments. These dot products are then fanned-out to update the remaining matrix coefficients in the same processor or saved in the buffer to be sent out to other processor during the parallel factorization phase.

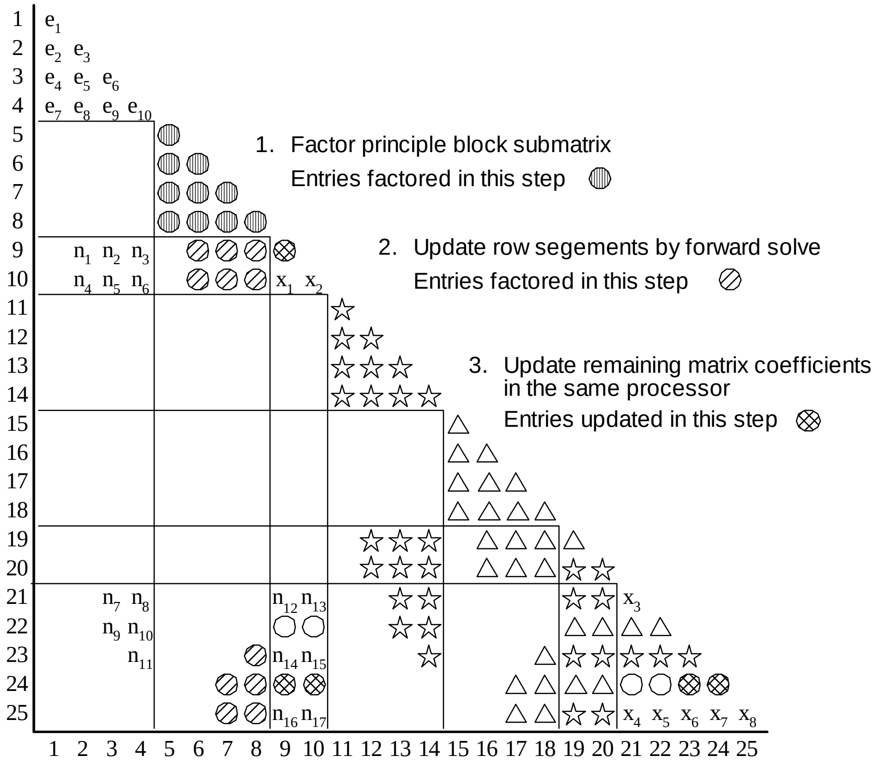
1. Factor principle block submatrix
Entries factored in this step
2. Update row segements by forward solve
Entries factored in this step
3. Update remaining matrix coefficients in the same processor
Entries updated in this step
e1 e2 e3 e4 e5 e6 e7 e8 e9 e10
n1 n2 n3 n4 n5 n6 n7 n8 n9 n10 n11 n12 n13 n14 n15 n16 n17
x1 x2 x3 x4 x5 x6 x7 x8
1 2 3 4 5 6 7 8 9 10 11 12 13 14 15 16 17 18 19 20 21 22 23 24 25

Figure 12. Phase One of Parallel Factorization

In the second phase of the numerical factorization, the column blocks shared by more than one processor are factorized. Figure 13 shows the parallel factorization procedures in this phase with the factor of matrix coefficients in Processor 1 being highlighted. The operations in this phase proceed as follows:

1. For the column blocks shared by multiple processors, each processor fans in the dot products generated in phase one of the numerical factorization. The principal block submatrix can be updated based on the received dot products.

2. Perform parallel factorization of column blocks. This step involves a parallel profile factorization of the principal block submatrix and updating the row segments shared by a group of processors. In this step, the processor responsible for the first row (say, row *r*) in the column block factorizes the row and broadcasts it to all other processors sharing the column block. The other processors receive the row factor and use it to update columns in them. The processor containing the next row, *r+1*, updates the row and broadcasts it to the other processors sharing the column block. The other processors continue receiving rows until it is time to factor a row they are responsible for. This process

continues until the entire submatrix is factored and all the row segments in the column block are updated.

3. After all the row segments in the column block have been updated, the row segments of the column blocks are circulated among the shared processors. After a processor receives another processor's row segment, the processor forms dot products between the row segments belonging to the two different processors. The row segment is then passed on to the next processor to update the matrix column blocks.

Note that in this parallel factorization strategy, the dot products between row segments are not fanned-in until the column blocks that needs the dot products is being factorized by the processors.

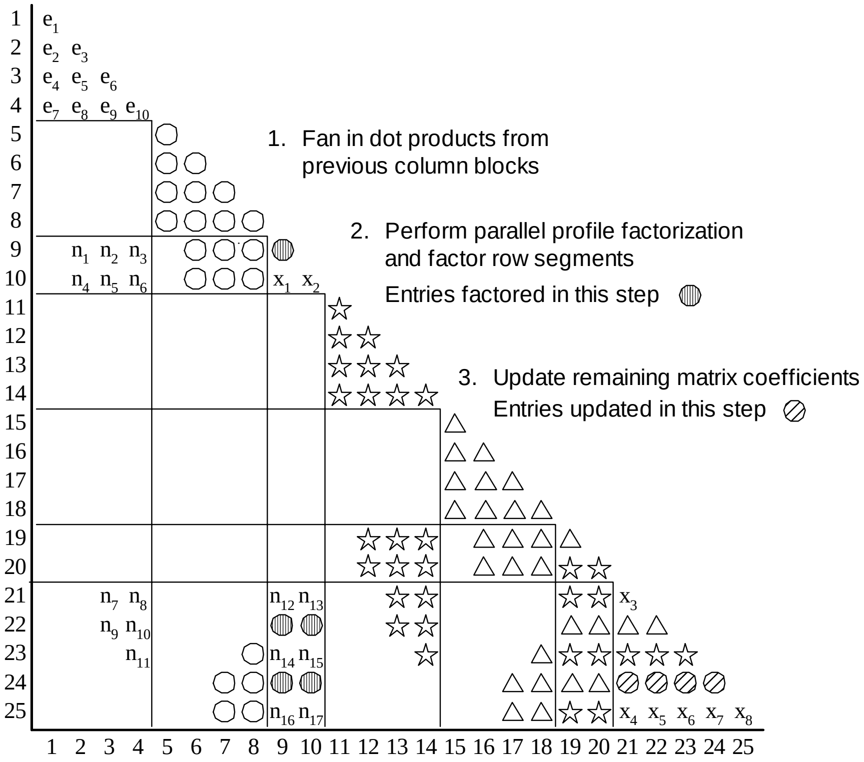

1. Fan in dot products from previous column blocks
2. Perform parallel profile factorization and factor row segments
Entries factored in this step ◍
3. Update remaining matrix coefficients
Entries updated in this step ⊘
e_1 e_2 e_3 e_4 e_5 e_6 e_7 e_8 e_9 e_{10}
n_1 n_2 n_3 n_4 n_5 n_6
x_1 x_2
n_7 n_8 n_9 n_{10} n_{11}
n_{12} n_{13} n_{14} n_{15} n_{16} n_{17}
x_3
x_4 x_5 x_6 x_7 x_8
1 2 3 4 5 6 7 8 9 10 11 12 13 14 15 16 17 18 19 20 21 22 23 24 25

Figure 13. Phase Two of Parallel Factorization

4.6 Parallel Numerical Solution

Following the parallel factorization is the parallel forward solution phase, which can be viewed symbolically as a procedure traversing the elimination tree from the leaves to the root. The solution vector *x* and the load vector *f* are divided into blocks just as the matrix is divided into column blocks determined by the elimination tree. The forward solution phase is also divided into two phases: a sequential phase and a parallel phase.

In the first phase, each processor calculates the blocks of *f* corresponding to the matrix blocks which reside entirely within a single processor. For each column block assigned to a processor, each processor performs a profile forward solve with the principal submatrix in the column block. Each processor also updates the shared portions of the solution vector based on the row segments that lie below the profile submatrices. The solution coefficients not assigned to this processor are stored in buffer to be sent to other processors.

Phase two of the parallel forward solution begins as the processors working together on the variables in the shared column blocks. There are three steps involved in this phase as outlined below:

1. The first step is to send and receive solution coefficients generated in phase one of the forward solution. These coefficients are used to update the partially solved block of solution vector *f*.

2. The second step performs parallel forward solution based on principal submatrix. As each value of *f* is calculated, for example *f* [*i*], it is broadcast to the other processors sharing the block. After receiving the value of *f* [*i*], the processor responsible for *f* [*i+1*] can complete the solution and broadcast the value to other processors sharing the column block. This process is repeated until the solution to the entire block is completed.

3. The third step is to use the values in this block to update other blocks using the rows segments in this column block.

Following the forward solution phase is the backward substitution procedure, which is essentially a reverse of the forward solution. The first phase of backward substitution deals with the portion of the solution vector shared by multiple processors and is essentially a reverse of the second phase of the forward solution. In the second phase, each processor calculates the portion of the solution vector corresponding to the column blocks residing within a single processor; the processors perform the calculations independently without any processor communications and may complete the solution at different times. Once all the processors finish the backward substitution, a global gathering function is invoked to obtain the global solution from each processor. This step is essential because each processor only has part of the global solution vector that it is responsible for.

5 Performance of ParCYCLIC

To demonstrate the simulation capability and parallel performance of ParCYCLIC, we have performed earthquake simulations for three-dimensional geotechnical models using ParCYCLIC. The simulations are performed on the Blue Horizon machine at San Diego Supercomputer Center. Blue Horizon is an IBM Scalable POWERparallel (SP) machine which has 144 compute nodes, each with 8 POWER3 RISC-based processors and with 4 GBytes of memory. Each processor on the node has equal shared access to the memory. The following presents the simulations of two 3D geotechnical finite element models.

5.1 Simulation of Pile-Soil Interaction in Liquefied Sloping Ground

Figure 14 shows a RPI centrifuge test model [42] to investigate the response of a single-pile foundation in a liquefied gently sloping ground, subjected to dynamic base excitation. The experiment was conducted using a rectangular, flexible-wall laminar box container (as shown in Figure 14). The soil profile consists of a saturated loose liquefiable sand layer (relative density Dr = 40%), underlain by a slightly cemented non-liquefiable sand layer [43]. The prototype single pile in the middle of the soil domain is 0.6m in diameter, 8m in length, and is free at the top. The model was inclined in 2 degrees and subjected to a predominantly 2Hz harmonic base excitation with a peak acceleration of 0.3g.

The centrifuge model is simulated using ParCYCLIC on Blue Horizon. The soil domain and the pile were discretized with 8-node brick elements, as shown in Figure 15. A half mesh configuration was used due to geometrical symmetry. ParCYCLIC is used to simulate the model for roughly 2200 time-steps. As shown from the results in Figures 16-18, good agreement has been achieved between the computed and the recorded acceleration, displacement, and pore pressure responses. Salient liquefaction response characteristics, including excess pore pressure generation and dissipation, acceleration spikes, pile lateral movement, and permanent soil lateral deformation, have been captured by the ParCYCLIC model with reasonable accuracy.

Table 1 summarizes the timing measurements for performing the simulation of the centrifuge test model on 8, 16, and 32 processors. Overall, significant decrease in both numerical factorization and the total execution time can be observed. Since there is no element duplication in the phases of the right-hand-side (RHS) formation and the stress update, these two procedures are scaled very well, or actually nearly linear, as shown in Table 1. In the hybrid element assignment strategy, element duplication occurs in the stiffness matrix formation. As the number of processors increases, the ratio of the duplicated portion (i.e., number of duplicated elements) over the non-duplicated portion becomes larger, and thus the parallel speedup of LHS formation decreases.

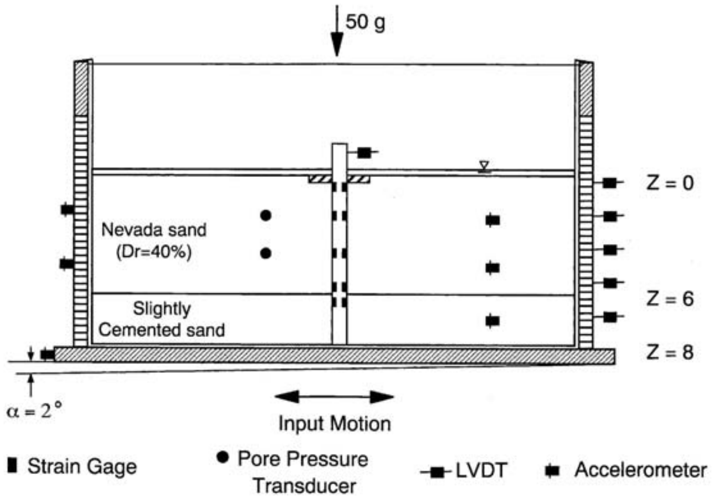

Figure 14. Lateral Spreading Pile Centrifuge Model in Two-Layer Soil Profile

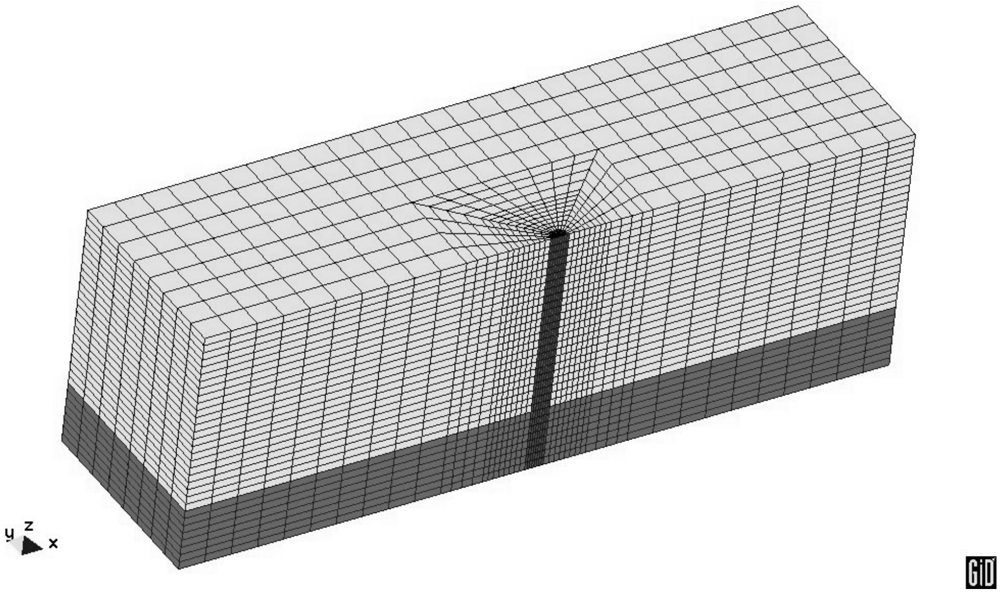

Figure 15. Finite Element Mesh for the Centrifuge Test Model

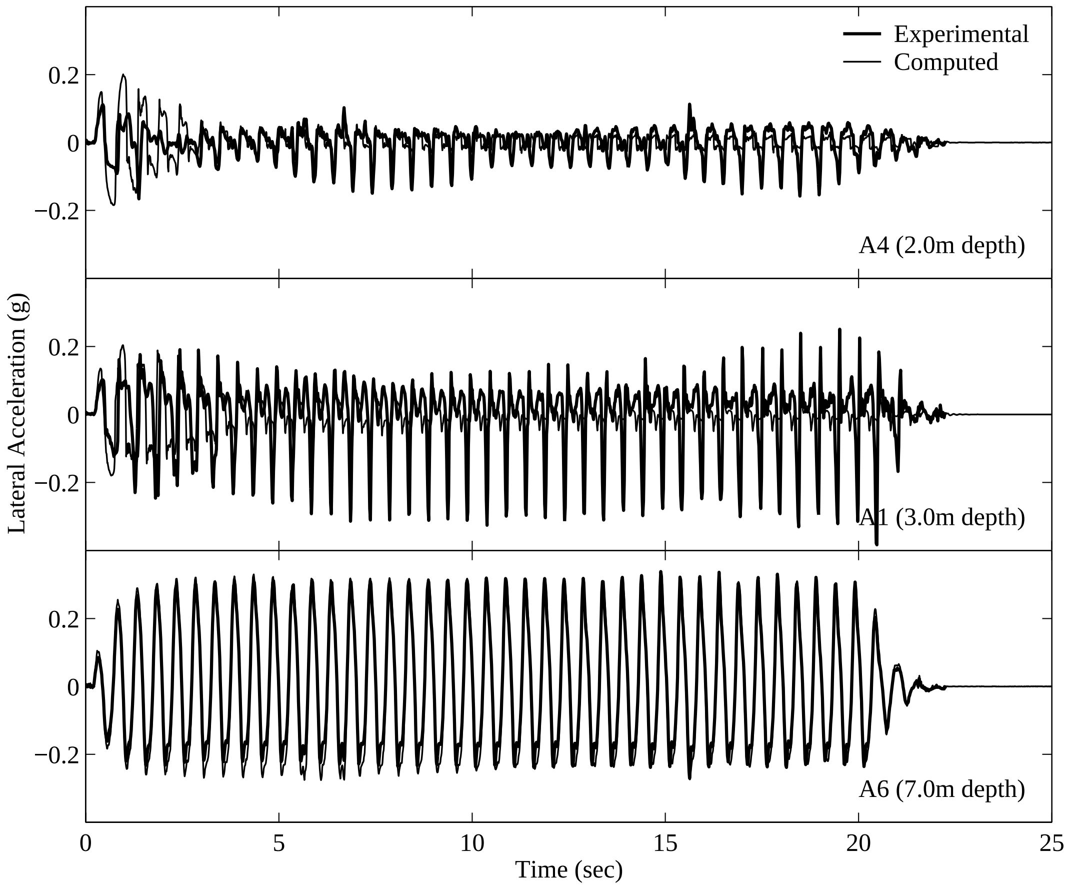

Figure 16. Computed and Recorded Lateral Acceleration Time Histories

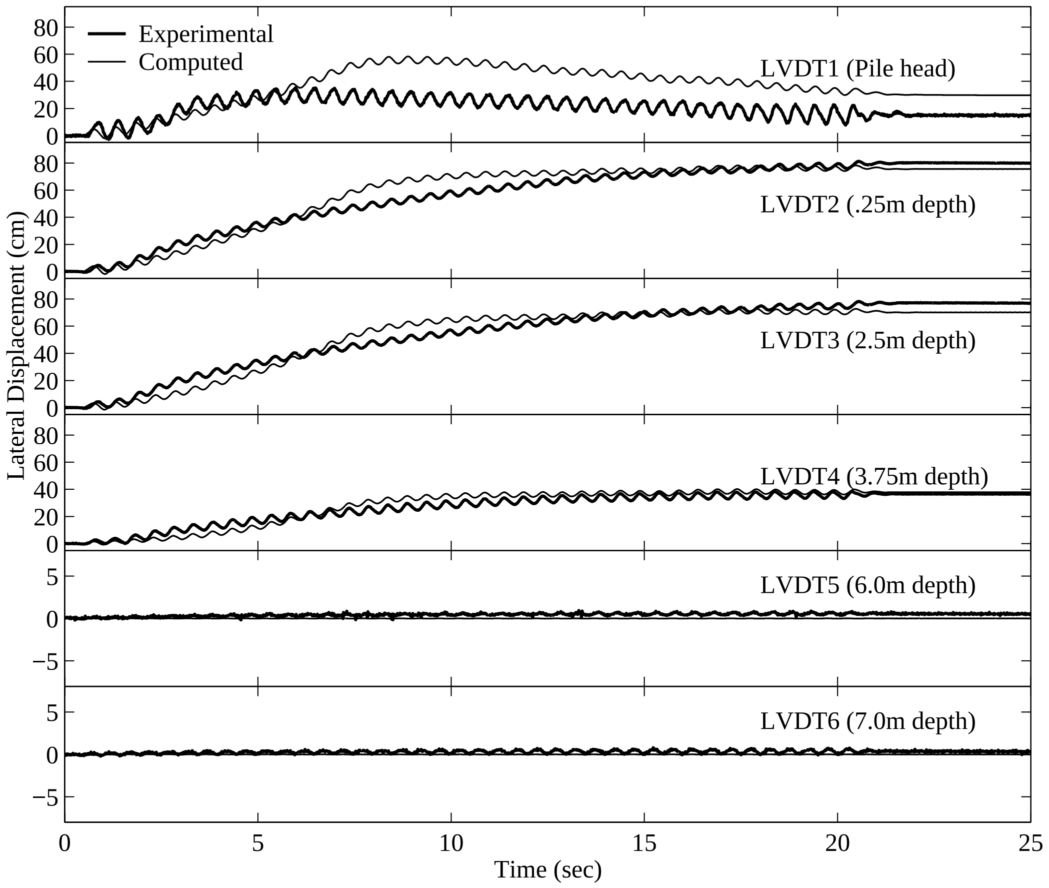

Figure 17. Computed and Recorded Pile Head and Soil Lateral Displacement Time Histories

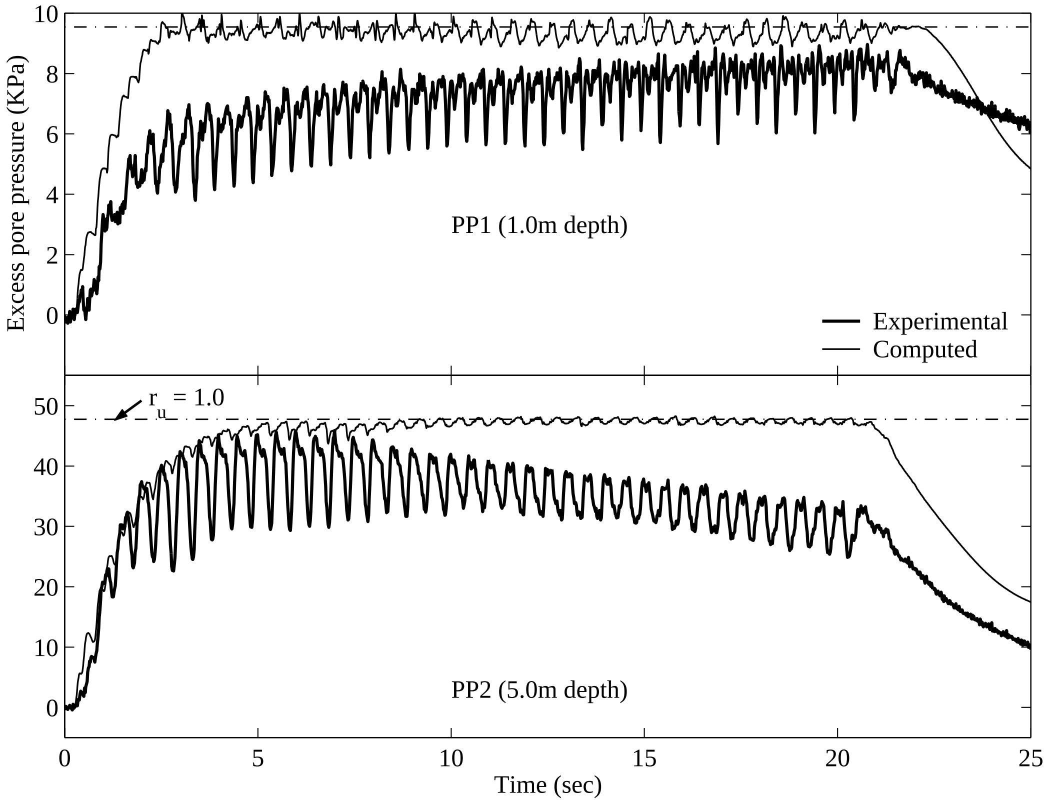

Figure 18. Computed and Recorded Excess Pore Pressure Time Histories

Table 1: Timing Measurements on the Simulation of the Centrifuge Model (time in second)

#procs	LHS formation	RHS formation	Stress update	Factorization	For. & back solve	Total Time
8	273.57	2446.79	254.42	2736.63	490.89	6406.25
16	164.10	1224.62	128.28	1491.37	341.37	3579.80
32	104.45	622.01	64.19	813.70	320.25	2157.35

The timing measurements on the initialization phase are shown in Table 2 in details. The initialization phase is essentially sequential and only consists of less than 2% of the total execution time. Most of the time in this phase was spent on the finite element model input, the adjacency structure formation, and the setup for matrix storage and the parallel solver indexing. The multilevel nested dissection ordering using METIS is relatively fast and less than 1 second is needed to order this finite element model with approximately 63,500 degrees of freedom. The times spent on the elimination tree setup and the symbolic factorization are insignificant comparing with the total execution time.

Table 2. Detailed Timing Results for the Initialization Phase (time in second).

#procs	8	16	32
Finite element mesh read-in	13.18		
Adjacency structure formation	9.38		
Multilevel nested dissection ordering (using METIS)	0.79		
Elimination tree setup and postordering	0.23		
Symbolic factorization	1.4		
Solver inter-processor communication setup	2.04	3.23	5.19
Matrix storage and solver indexing setup	14.74	9.72	4.11
Total on initialization phase	45	41.78	38.53

5.2 Stone Column Centrifuge Test Model

The second example is a stone-column centrifuge test model, as shown in Figure 19. Again, half mesh is used due to its geometrical symmetry. Many of the past earthquake-induced ground failures and large deformations observed in the built-environment have occurred mostly in sites containing non-plastic silty soils. One of the improved remediation techniques to mitigate liquefaction hazards in these silty soils is installing stone columns [44]. In the stone column test model, a number of gravel columns are embedded into a fully-saturated soil foundation filled with silt. The model is then subjected to earthquake excitation along the x-direction at the base.

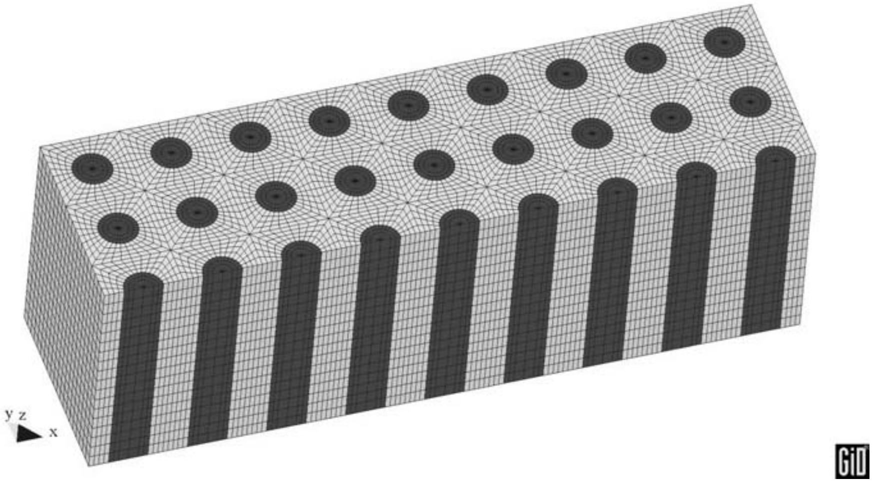

Figure 19. Finite Element Model of the Stone Column Centrifuge Test

Since the simulation of this model requires significant computer resources, only one time step is performed to show the parallel performance of ParCYCLIC. Table 3 summarizes the timing results of the solution phase, the LDL^T numerical factorization, the forward and backward solutions, and the total execution time (which includes the initialization phase) for one time step. The parallel speedup and the total execution times for the solution phase are also shown in Table 3. Note that the stone column model, with a scale of 364,800 degrees of freedom, cannot fit into the memory of less than 4 processors. As shown in Table 3 and Figure 20, excellent parallel speedup is achieved for this model.

Table 3. Solution Times for the Stone Column Centrifuge Test Model (time in seconds)

Number of processors	LDL^T factorization	Forward and backward solve	Solution phase	Total execution time
4	1246.08	2.76	1306.87	1769.00
8	665.66	1.56	702.09	1150.17
16	354.99	0.98	378.35	841.38
32	208.90	0.67	225.93	668.02
64	125.05	0.66	142.33	583.98

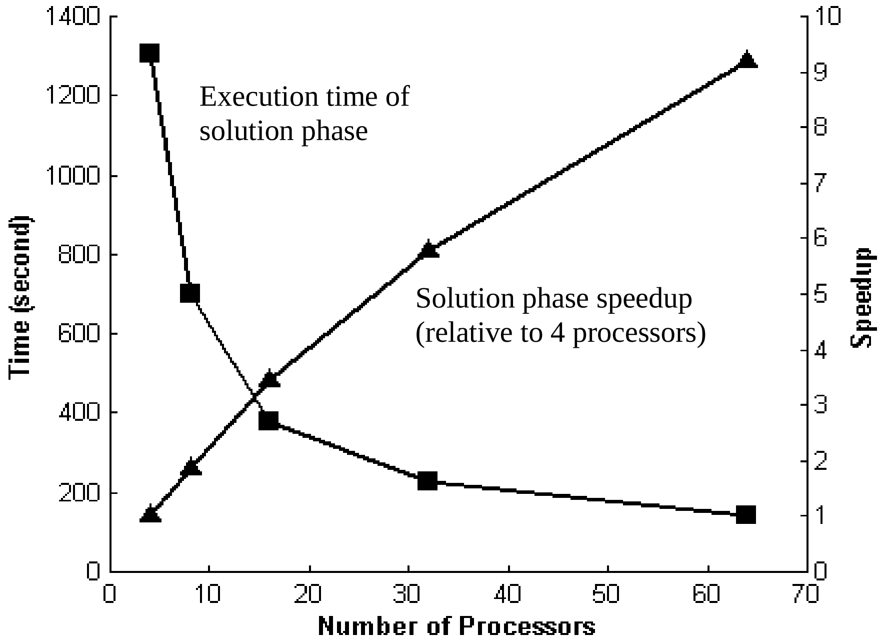

Figure 20. Execution Times and Speedup of the Solution Phase for the Stone Column Model

6 Conclusions

This paper presents the analysis and solution strategies employed in ParCYCLIC, a parallel nonlinear finite element program for the simulations of earthquake site response and liquefaction. In ParCYCLIC, finite elements are employed within an incremental plasticity, coupled solid-fluid formulation. A constitutive model developed for the simulation of liquefaction-induced deformations is a main component of this analysis framework. Extensive calibration of ParCYCLIC has been conducted with results from experiments and full-scale response of earthquake simulations involving ground liquefaction.

The solution strategy in ParCYCLIC is based on a parallel sparse solver [7]. Several improvements have been made to the original parallel sparse solver. An automatic domain decomposer is used to partition the finite element mesh so that the workload on each processor is more or less evenly distributed and the communication among processors is minimized. METIS routines [33] are incorporated in ParCYCLIC to perform domain decomposition, and the internal nodes of each sub-domain are ordered using Multilevel Nested Dissection or other ordering strategies. Because of the automatic domain decomposer, the input file for ParCYCLIC is very easy to prepare. It does not contain any information for processor assignment of nodes and elements, and essentially has the same format as the input file for the sequential program CYCLIC. Moreover, a parallel data structure is introduced to store the matrix coefficients. There are three different data structures for storing the coefficients of the matrix: one for the principal block submatrices associated with the column blocks assigned to a single processor, one for the principal block submatrices associated with column blocks shared by multiple processors, and one for the row segments in column blocks. An enhancement to the original parallel solver is the processor communication interface. The original solver is designed for running on Intel supercomputers such as the hypercube, the Delta system and the Intel Paragon; and the message-passing routines are written using the Intel NX library [45]. The communication in ParCYCLIC is written in MPI [31]; this makes ParCYCLIC more portable to run on a wide range of parallel computers and workstation clusters.

Large-scale experimental results for 3-D geotechnical simulations have been presented to demonstrate the capability and performance of ParCYCLIC. Simulation results demonstrated that ParCYCLIC is suitable for large-scale geotechnical simulations, and good agreement has been achieved between the computed and the recorded acceleration, displacement, and pore pressure responses. Excellent parallel speedup has also been obtained from the simulation results. Last but not least, it is shown that ParCYCLIC program, which employs direct solution scheme, remains scalable to a large number of processors, e.g., 64 or more.

Acknowledgements

This research was supported in part by the National Science Foundation, Grant Number CMS-0084616 to University of California, San Diego, and Grant Number CMS-0084530 to Stanford University. Additional funding was provided in part by the Pacific Earthquake Engineering Research (PEER) Center, under the National Science Foundation Award Number EEC-9701568. Thanks to Dr. Zhaohui Yang at University of California, San Diego for his assistance with the development of the original CYCLIC program. This research was also supported in part by NSF cooperative agreement ACI-9619020 through computing resources provided by the National Partnership for Advanced Computational Infrastructure at the San Diego Supercomputer Center.

References

1. Gummadi LNB, Palazotto AH. Nonlinear finite element analysis of beams and arches using parallel processors. *Computers and Structures* 1997; **63**:413-428.

2. Amestoy PR, Duff IS, L'Excellent J-Y. Multifrontal parallel distributed symmetric and unsymmetric solvers. *Computer Methods in Applied Mechanics and Engineering* 2000; **184**(2-4):501-520.

3. Li XS, Demmel JW. Making sparse Gaussian elimination scalable by static pivoting. *Proceedings of SC98: High Performance Networking and Computing Conference*. Orlando, FL, 1998.

4. Heath MT, Ng E, Peyton BW. Parallel algorithms for sparse linear systems. *SIAM Review* 1991; **33**(3):420-460.

5. George A, Heath MT, Liu J, Ng E. Solution of sparse positive definite systems on a shared-memory multiprocessor. *International Journal of Parallel Programming* 1986; **15**(4):309-328.

6. George A, Heath MT, Liu J, Ng E. Solution of sparse positive definite systems on a hypercube. *Journal of Computational and Applied Mathematics* 1989; **27**(1-2):129-156.

7. Law KH, Mackay DR. A parallel row-oriented sparse solution method for finite element structural analysis. *International Journal for Numerical Methods in Engineering* 1993; **36**(17):2895-2919.

8. Watson BC, Noor AK. Nonlinear structural analysis on distributed-memory computers. *Computers and Structures* 1996; **58**(2):233-247.

9. Nikishkov GP, Kawka M, Makinouchi A, Yagawa G, Yoshimura S. Porting an industrial sheet metal forming code to a distributed memory parallel computer. *Computers and Structures* 1998; **67**(6):439-449.

10. Romero ML, Miguel PF, Cano JJ. A parallel procedure for nonlinear analysis of reinforced concrete three-dimensional frames. *Computers and Structures* 2002; **80**(16-17):1337-1350.

11. Modak S, Sotelino ED. An object-oriented programming framework for the parallel dynamic analysis of structures. *Computers and Structures* 2002; **80**(1):77-84.

12. McKenna F. Object-oriented finite element programming: Frameworks for analysis, algorithm and parallel computing. *Ph.D. Thesis*, University of California at Berkeley, Berkeley, CA 1997.

13. Krysl P, Bittnar Z. Parallel explicit finite element solid dynamics with domain decomposition and message passing: Dual partitioning scalability. *Computers and Structures* 2001; **79**(3):345-360.

14. Bao H, Bielak J, Ghattas O, O'Hallaron DR, Kallivokas LF, Shewchuk JR, Xu J. Earthquake ground motion modeling on parallel computers. *Proceedings of ACM/IEEE Supercomputing Conference*. Pittsburgh, PA, 1996.

15. Parra E. Numerical modeling of liquefaction and lateral ground deformation including cyclic mobility and dilation response in soil systems. *Ph.D. Thesis*, Rensselaer Polytechnic Institute, Troy, NY 1996.

16. Yang Z, Elgamal A. Influence of permeability on liquefaction-induced shear deformation. *Journal of Engineering Mechanics, ASCE* 2002; **128**(7):720-729.

17. Chan AHC. A unified finite element solution to static and dynamic problems in geomechanics. *Ph.D. Thesis*, University of Wales, Swansea, U.K. 1988.

18. Zienkiewicz OC, Chan AHC, Pastor M, Paul DK, Shiomi T. Static and dynamic behavior of soils: A rational approach to quantitative solutions: I. Fully saturated problems. *Proceedings of the Royal Society London, Series A, Mathematical and Physical Sciences* 1990; **429**:285-309.

19. Yang Z. Numerical modeling of earthquake site response including dilation and liquefaction. *Ph.D. Thesis*, Columbia University, New York, NY 2000.

20. Biot MA. The mechanics of deformation and acoustic propagation in porous media. *Journal of Applied Physics* 1962; **33**(4):1482-1498.

21. Elgamal A, Yang Z, Parra E, Ragheb A. Modeling of cyclic mobility in saturated cohesionless soils. *International Journal of Plasticity* 2003; **19**(6):883-905.

22. Prevost JH. A simple plasticity theory for frictional cohesionless soils. *International Journal of Soil Dynamics and Earthquake Engineering* 1985; **4**(1):9-17.

23. Elgamal A, Yang Z, Parra E. Computational modeling of cyclic mobility and post-liquefaction site response. *Journal of Soil Dynamics and Earthquake Engineering* 2002; **22**(4):259-271.

24. Elgamal A, Parra E, Yang Z, Adalier K. Numerical analysis of embankment foundation liquefaction countermeasures. *Journal of Earthquake Engineering* 2002; **6**(4):447-471.

25. Ishihara K, Tatsuoka F, Yasua S. Undrained deformation and liquefaction of sand under cyclic stresses. *Soils and Foundations* 1975; **15**(1):29-44.

26. Mroz Z. On the description of anisotropic work hardening. *Journal of Mechanics and Physics of Solids* 1967; **15**(1):163-175.

27. Mackay DR. Solution methods for static and dynamic structural analysis on distributed memory computers. *Ph.D. Thesis*, Stanford University, Stanford, CA 1992.

28. Herndon B, Aluru N, Raefsky A, Goossens RJG, Law KH, Dutton RW. A methodology for parallelizing pde solvers: Applications to semiconductor device simulation. *Proceedings of the Seventh SIAM Conference on Parallel Processing for Scientific Computing*. San Francisco, CA, 1995.

29. Law KH. Large scale engineering computations on distributed memory parallel computers and distributed workstations. *Proceedings of NSF Workshop on Scientific Supercomputing, Visualization and Animation in Geotechnical Earthquake Engineering and Engineering Seismology*. Carnegie-Mellon University, Pittsburgh, PA, 1994.

30. Aluru NR. Parallel and stabilized finite element methods for the hydrodynamic transport model of semiconductor devices. *Ph.D. Thesis*, Stanford University, Stanford, CA 1995.

31. Snir M, Gropp W. *MPI: The complete reference*. MIT Press: Boston, MA, 1998.

32. Fahmy MW, Namini AH. A survey of parallel nonlinear dynamic analysis methodologies. *Computers and Structures* 1994; **53**(4):1033-1043.

33. Karypis G, Kumar V. *METIS version 4.0: A software package for partitioning unstructured graphs, partitioning meshes, and computing fill-reducing orderings of sparse matrices*. Department of Computer Science and Engineering, University of Minnesota, 1998

34. Karypis G, Kumar V. A fast and high quality multilevel scheme for partitioning irregular graphs. *SIAM Journal on Scientific Computing* 1998; **20**(1):359-392.

35. Karypis G, Kumar V. Multilevel k-way partitioning scheme for irregular graphs. *Journal for Parallel and Distributed Computing* 1998; **48**(1):96-129.

36. George A. Computer implementation of the finite element method. *Ph.D. Thesis*, Stanford University, Stanford, CA 1971.

37. Tinney WF, Walker JW. Direct solutions of sparse network equations by optimally ordered triangular factorization. *Proceedings of the IEEE* 1967; **55**(11):1801-1809.

38. Lipton RJ, Rose DJ, Tarjan RE. Generalized nested dissection. *SIAM Journal on Numerical Analysis* 1979; **16**(1):346-358.

39. Liu JWH. The role of elimination trees in sparse factorization. *SIAM Journal on Matrix Analysis and Applications* 1990; **11**(1):134-172.

40. Law KH, Fenves SJ. A node-addition model for symbolic factorization. *ACM Transactions on Mathematical Software* 1986; **12**(1):37-50.

41. Liu JWH. A generalized envelope method for sparse factorization by rows. *ACM Transactions on Mathematical Software* 1991; **17**(1):112-129.

42. Abdoun T. Modeling of seismically induced lateral spreading of multi-layered soil and its effect on pile foundations. *Ph.D. Thesis*, Rensselaer Polytechnic Institute, Troy, NY 1997.

43. Abdoun T, Doubry R. Evaluation of pile foundation response to lateral spreading. *Soil Dynamics and Earthquake Engineering* 2002; **22**(9-12):1069-1076.

44. Pekcan G, Yen WP, Friedland IM. Seismic vulnerability study of highway systems: Tea-21 research project. *Proceedings of 15th U.S.-Japan Bridge Engineering Workshop*. Tsukuba, Japan, 1999.

45. Pierce P, Regnier G. The paragon implementation of the NX message passing interface. *Proceedings of the Scalable High Performance Computing Conference (SHPCC94)*. Knoxville, TN, 1994.